© 2016 IEEE. Personal use of this material is permitted. Permission from IEEE must be obtained for all other uses, in any current or future media, including reprinting/republishing this material for advertising or promotional purposes, creating new collective works, for resale or redistribution to servers or lists, or reuse of any copyrighted component of this work in other works.

Performance and Reliability Comparison of 1T-1R RRAM arrays with Amorphous and Polycrystalline HfO_2

Alessandro Grossi*, Eduardo Perez†, Cristian Zambelli*, Piero Olivo*, and Christian Wenger†
*Università degli Studi di Ferrara, Dip. di Ingegneria, ENDIF, Via G. Saragat 1, 44122 Ferrara, Italy
†IHP, Im Technologiepark 25, 15236 Frankfurt (Oder), Germany

E-mail: alessandro.grossi@unife.it

***Abstract*—In this work, a comparison between 1T-1R RRAM 4kbits arrays manufactured either with amorphous or polycrystalline HfO_2 in terms of performance, reliability, Set/Reset operations energy requirements, intra-cell and inter-cell variability during 10k Set/Reset cycles is reported. Polycrystalline array shows higher current ratio, lower switching voltages, lower power consumption, minor endurance degradation and higher overall yield than amorphous array. The drawbacks are represented by the higher Forming voltage, the larger read current distribution after Forming and the higher Reset voltage dispersion.**

I. Introduction

Resistive Random Access Memories (RRAM) technology gathered significant interest for several applications [1]–[3]. RRAM behavior is based on the possibility of electrically modifying the conductance of a Metal-Insulator-Metal (MIM) stack: the Set operation moves the cell in a low resistive state (LRS), whereas Reset brings the cell in a high resistive state (HRS) [4], [5]. To activate such a switching behavior, some technologies require a preliminary Forming operation [6]–[8].

The choice of a proper MIM technology for RRAM cells, exhibiting good uniformity and low switching voltages, is therefore a key issue for array structures fabrication and reliable electrical operation [9]. Such a process step is mandatory to bring this technology to a maturity level. In this work, a comparison between 1T-1R RRAM 4kbits arrays manufactured either with amorphous [5] or polycrystalline [10] HfO_2 is performed. In amorphous HfO_2 the conduction mainly occurs through a conductive filament created during the Forming operation with highly variable concentration of defects, whereas in polycristalline HfO_2 the conduction occurs only through grain boundaries with a very low defect concentration. These differences in terms of conduction properties and defect concentrations translate into different switching properties [9], with several implications on inter-cell (variations between cells) and intra-cell (cycle-to-cycle variations of any given cell) variability. In this work a comparison in terms of performance, reliability, Set/Reset operations energy requirements, intra-cell and inter-cell variability during 10k endurance cycles is reported.

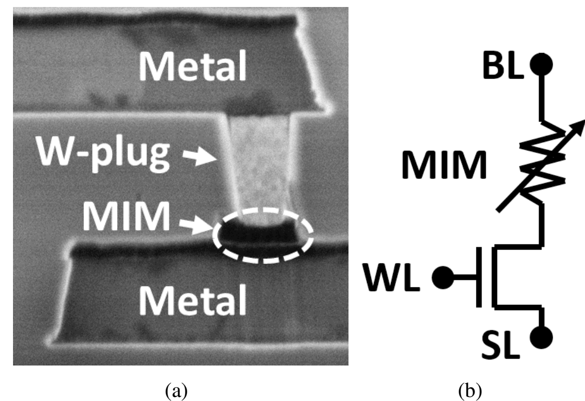

(a) (b)

Fig. 1. Cross-sectional STEM image (a) and schematic (b) of the 1T-1R cell integrated in the arrays.

II. Experimental Setup

The 1T-1R memory cells in the 4kbits arrays are constituted by a select NMOS transistor manufactured with a 0.25 μm BiCMOS technology whose drain is in series to the MIM stack. The wordline (WL) voltage applied to the gate of the NMOS transistor allows setting the cell current compliance. The cross-sectional Scanning Transmission Electron Microscopy (STEM) image of the cell and the 1T-1R cell schematic are reported in Fig. 1. The variable MIM resistor is composed by 150 nm TiN top and bottom electrode layers deposited by magnetron sputtering, a 7 nm Ti layer, and a 8 nm HfO_2 layer deposited with two different Atomic Vapour Deposition (AVD) processes resulting either in amorphous (A) or polycrystalline (P) HfO_2 films, respectively. The resistor area is equal to 0.4 μm^2. For amorphous films it has been integrated also a resistor with larger area that shows improved reliability and performance (i.e., 1 μm^2) [4]. The Forming/Set/Reset operations on the arrays were performed by using an Incremental Pulse and Verify algorithm [11]. The bitline (BL), sourceline (SL) and WL voltages applied during Forming, Set, Reset and Read operations are reported in Tab. I. Reset operations were performed by applying the WL voltage that allows maximizing the cells switching yield

This is the accepted version of the paper. The published version can be found at ieeexplore.ieee.org/abstract/document/7440057/
The DOI of the published version is: 10.1109/ULIS.2016.7440057

TABLE I
FORMING, SET, RESET AND READ VOLTAGE PARAMETERS.

Operation	V_{SL} [V]	V_{BL} [V]	V_{WL} [V]
Forming	0	2-3.2	1.5
Set	0	0.2-3.2	1.5
Reset	0.2-3.2	0	2.5 (A)/ 2.8 (P)
Read	0	0.2	1.5

(2.8 V on array A and 2.5 V on array P) while avoiding the breakdown of the HfO_2 [12]. Pulses were applied during Forming by increasing V_{BL} with ΔV_{BL}=0.01V, whereas during Set and Reset ΔV_{BL}=0.1V and ΔV_{SL}=0.1V have been used, respectively. Each pulse featured a duration of 10μs, with a rise/fall time of 1μs to avoid overshoot issues. Set operation was stopped on a cell when the read-verify current reached at least 20μA, whereas Reset was stopped when reached al least 10μA. Forming, Set and Reset BL/SL voltages necessary to reach the requested read-verify current targets are extracted from the characterization data and labelled as V_{FORM}, V_{SET}, and V_{RES}, respectively.

III. EXPERIMENTAL RESULTS

1T-1R cell arrays integrated with A-HfO_2 (A-array) with small (0.4 μm^2) and large (1 μm^2) resistor area, and P-HfO_2 (P-array) resulted in a Forming Yield (calculated as the cell percentage having a read verify current after forming $I_{read} \geq 20\mu A$) of 58%, 90%, and 95%, respectively. Fig. 2 shows the average current ratios between Low Resistive State (LRS) and High Resistive State (HRS) read currents (I_{LRS}/I_{HRS}), calculated on the entire cells population during Set/Reset cycling, and their relative dispersion coefficient. The dispersion coefficient, defined as (σ^2/μ), has been used to evaluate the cell-to-cell variability. The minimum current ratio that allows to correcly discriminate between HRS and LRS ($I_{LRS}/I_{HRS} > 2$) is indicated for comparison purposes [5]. Due to the faster cell degradation, the average ratios of A-arrays with resistor area of 0.4 μm^2 and 1 μm^2 cross the minimum ratio limit after 200 and 1k cycles, respectively. P-array showed higher ratio ($\approx$ 2.8) even after 10k cycles, but also a higher dispersion coefficient after Forming (i.e., cycle 1). The grain boundaries conduction mechanism in the polycrystalline HfO_2 structure could be the reason of the higher cell-to-cell variability in P-arrays [13]. A-array with resistor area of 1 μm^2 shows a slightly higher average ratio and a slower degradation than A-array with resistor area of 0.4 μm^2. In smaller cells the presence of defects in the HfO_2 stack has a stronger impact on the performance since makes the switching operations more difficult to control, speeds up the degradation and increases the overall inter-cell variability [14].

Fig. 3 shows a comparison between I_{LRS} and I_{HRS} cumulative distributions measured at cycle 1 and after the 10k Set/Reset cycling test: A-arrays show more compact distributions at cycle 1, however after cycling P-array shows a higher percentage of correctly switching cells reaching the Set/Reset verify targets. I_{HRS} cumulative distribution in P-array shows a larger distribution tail at cycle 1 compared to A-arrays. After 10k cycles the cells degradation makes more difficult to break or re-create the filament, hence the voltage requested to reach the verify target increases as well as the number of cells not able to reach the verify target. An enlargement of the upper tail in P-array HRS distribution can be observed whereas on A-arrays a strong shift of the distributions towards higher currents occurs, since a higher number of cells is not able reach the Reset threshold. The reason of the lower ratio in A-array with small resistor area can be explained by the cumulative distributions, since they show lower I_{LRS} and higher I_{HRS} than cells with larger resistor area either at cycle 1 and after

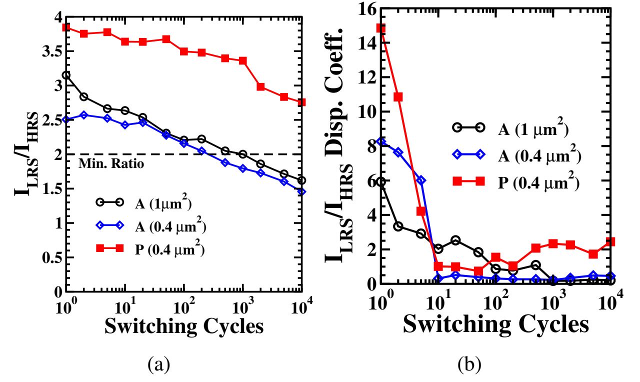

Fig. 2. I_{LRS}/I_{HRS} current ratio average values (a) and dispersion coefficients (b) calculated during cycling.

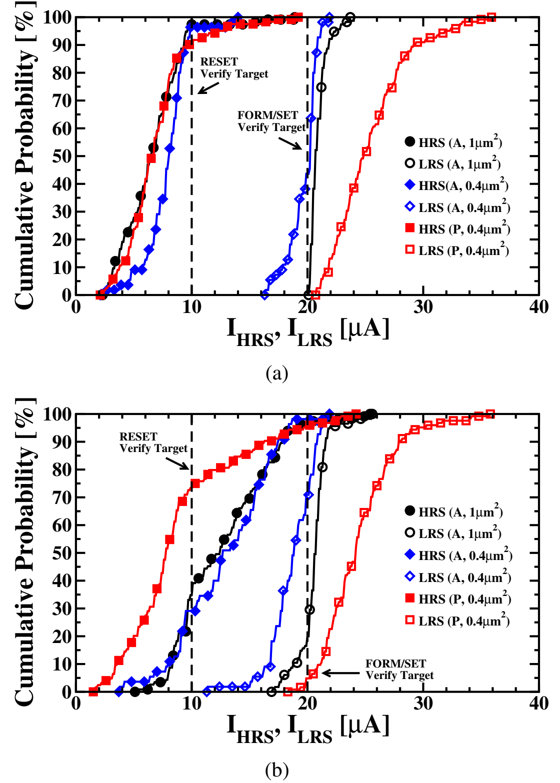

Fig. 3. I_{HRS} and I_{LRS} cumulative distributions at cycle 1 (a) and at cycle 10k (b).

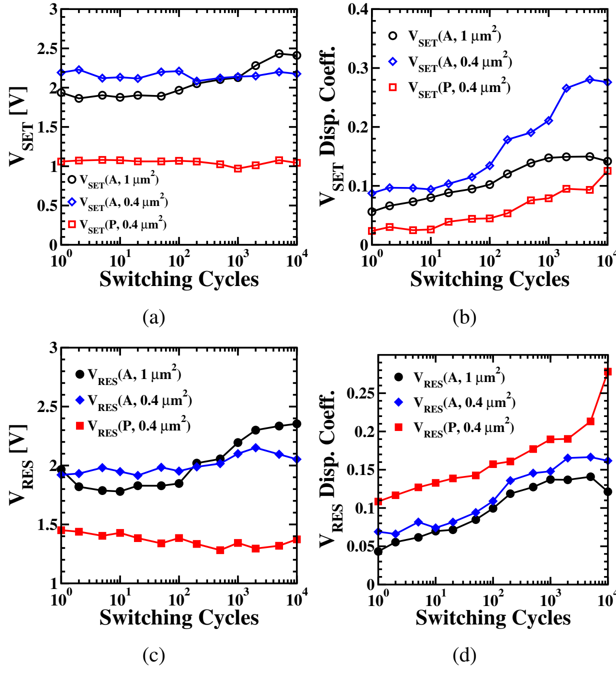

Fig. 4. V_{SET} and V_{RES} average values (a,c) and dispersion coefficients (b,d) calculated during cycling.

10k cycles. In I_{LRS} cumulative distributions the cells not able to reach the Set verify target generate a lower tail on P-arrays after 10k cycles, whereas on A-arrays a higher number of cells is not able to reach the Set verify target especially when cells with resistor area of 0.4 μm^2 are considered. This results into a strong shift of the distributions towards lower currents, especially in A-array with small resistor area that shows a high number of cells not reaching the Set verify target even at cycle 1.

Fig. 4 shows the average Set and Reset switching voltages (V_{SET}, V_{RES}) and their relative dispersion coefficients: lower V_{SET} and V_{RES} are required on P-array which also shows no variations during Set/Reset cycling, whereas V_{SET}, V_{RES} increase on A-arrays during cycling. V_{RES} on P-array shows the highest variability: such operation is critical and very difficult to control in RRAM arrays since it strongly depends on how the filament is created: over Forming, as well as endurance degradation, can make the filament difficult to disrupt, increasing the V_{RES} variability [11]. A-arrays show similar behavior of the average V_{SET} and V_{RES} (a lower average V_{SET} is observed on A-array with larger resistor area only up to 500 cycles), while a higher V_{SET} and V_{RES} dispersion can be observed in A-array with smaller resistor area.

Fig. 5 shows the cumulative distributions of switching voltages during Forming, while Fig. 6 shows the Set and Reset switching voltages cumulative distributions at cycle 1 and after the Set/Reset cycling. Forming, Set and Reset incremental pulse algorithms starting point and last attempt are indicated, corresponding to the first and the last voltage pulse available in the incremental pulse and verify procedure [11]. P-array requires lower V_{SET} and V_{RES} but higher V_{FORM} if compared to A-array with the same resistor area. A-array with larger resistor area requires higher V_{FORM}. Moreover, it can be observed that ≈ 40% of the devices with smaller resistor area reached the forming threshold at V_{FORM}=2 V, corresponding to the first attempt of the Forming Algorithm. Since P-array shows a more compact distribution on V_{SET} and a larger V_{RES} than A-arrays, faster Set operation could be reliably used on P-array, whereas on Reset an incremental pulse with verify technique is required to ensure good reliability. A-arrays show large distributions on both V_{SET} and V_{RES}, hence the adaptation of incremental pulse with verify techniques is mandatory on such arrays.

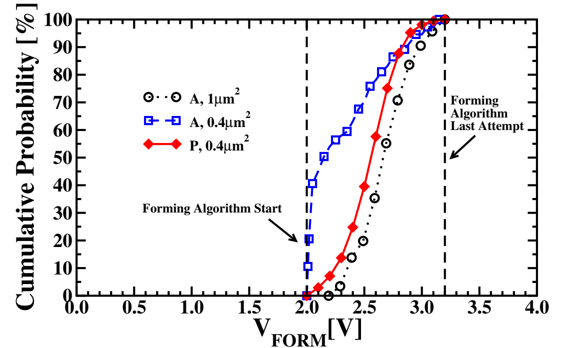

Fig. 5. V_{FORM} cumulative distributions.

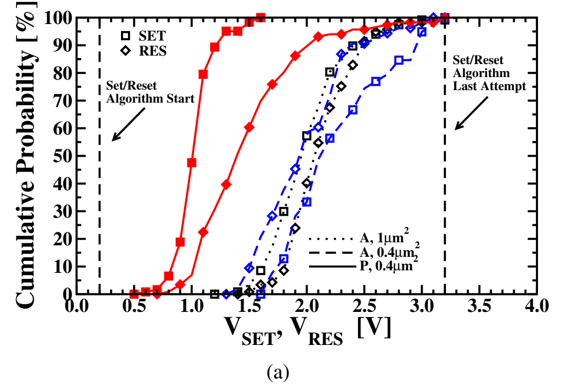

(a)

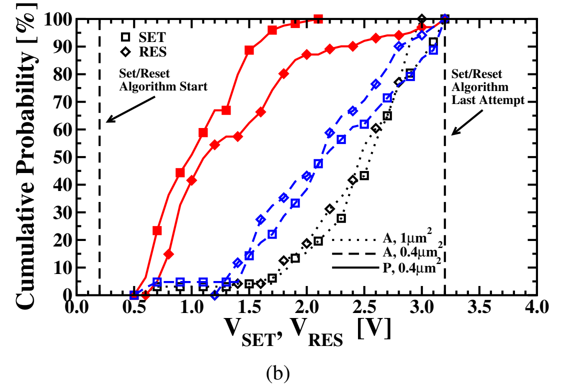

(b)

Fig. 6. V_{SET} and V_{RES} cumulative distributions at cycle 1 (a) and at cycle 10k (b).

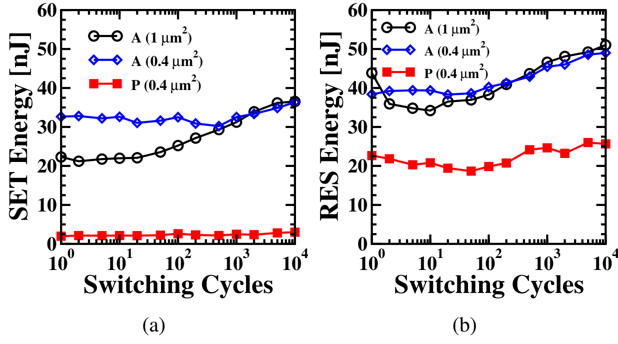

Fig. 7. Energy required to perform Set (a) and Reset (b) operations as a function of the Set/Reset cycle number.

Fig. 7 shows the average energy required to perform Set and Reset operations on a single cell. The overall energy required to create/disrupt the conductive filament during Set/Reset operations has been calculated as [11]:

$$E = \sum_{i=1}^{n} V_{pulse,i} * I_{pulse,i} * T_{pulse} + V_{read} * I_{read,i} * T_{read} \quad (1)$$

Where n is the number of reset pulses applied during incremental pulse operation, $V_{pulse,i}$ is the pulse voltage applied at step i, $I_{pulse,i}$ is the current flowing through RRAM cell during pulse i application, $T_{pulse} = 10\mu s$ is the pulse length, V_{read} =0.2 V is the read voltage applied during verify operation, $I_{read,i}$ is the current read on the RRAM during read verify step i, and $T_{read} = 10\mu s$ is the verify pulse length. P-array shows lower power consumption with a lower increase during cycling thanks to a lower V_{SET} and V_{RES}. A-arrays with different resistor area show similar power consumption during Reset operation, whereas a lower consumption during Set is observed on A-array with larger resistor area only up to 500 cycles since cells with larger resistor area require lower V_{SET}.

IV. Conclusions

1T-1R RRAM arrays manufactured with P-HfO_2 shows several advantages compared to A-HfO_2 even considering their improved process: higher current ratio, lower switching voltages, lower power consumption, minor endurance degradation and higher overall yield. Moreover, P-array show very low V_{SET} variability, hence faster Set operation could be reliably performed. P-array disadvantages are represented by the larger HRS distribution after Forming, the higher Reset voltage dispersion and the higher V_{FORM} if compared to A-array with the same resistor area, however but it must be pointed out that Forming operation is performed only once. The grain boundaries conduction mechanism in the polycrystalline HfO_2 structure could be the reason of the higher cell-to-cell variability in P-arrays.

Acknowledgments

This work was supported by the European Union's H2020 research and innovation programme under grant agreement N° 640073.

References

[1] S. Tanachutiwat, M. Liu, and W. Wang, "FPGA Based on Integration of CMOS and RRAM," *IEEE Trans. on Very Large Scale Integration (VLSI) Systems*, vol. 19, no. 11, pp. 2023–2032, Nov 2011.

[2] D. Garbin, E. Vianello, O. Bichler, Q. Rafhay, C. Gamrat, G. Ghibaudo, B. DeSalvo, and L. Perniola, "HfO2-Based OxRAM Devices as Synapses for Convolutional Neural Networks," *IEEE Trans. on Electron Devices*, vol. 62, no. 8, pp. 2494–2501, Aug 2015.

[3] T. Xu and V. Leppanen, "Analysing emerging memory technologies for big data and signal processing applications," in *Digital Information Processing and Communications (ICDIPC), 2015 Fifth International Conference on*, Oct 2015, pp. 104–109.

[4] C. Zambelli, A. Grossi, D. Walczyk, T. Bertaud, B. Tillack, T. Schroeder, V. Stikanov, P. Olivo, and C. Walczyk, "Statistical analysis of resistive switching characteristics in ReRAM test arrays," in *IEEE Int. Conf. on Microelectronics Test Structures (ICMTS)*, Mar 2014, pp. 27–31.

[5] C. Zambelli, A. Grossi, P. Olivo, D. Walczyk, J. Dabrowski, B. Tillack, T. Schroeder, R. Kraemer, V. Stikanov, and C. Walczyk, "Electrical characterization of read window in ReRAM arrays under different SET/RESET cycling conditions," in *IEEE Int. Memory Workshop (IMW)*, May 2014, pp. 1–4.

[6] D. Walczyk, T. Bertaud, M. Sowinska, M. Lukosius, M. A. Schubert, A. Fox, D. Wolansky, A. Scheit, M. Fraschke, G. Schoof, C. Wolf, R. Kraemer, B. Tillack, R. Korolevych, V. Stikanov, C. Wenger, T. Schroeder, and C. Walczyk, "Resistive switching behavior in TiN/HfO_2/Ti/TiN devices," in *Int. Semiconductor Conf. Dresden-Grenoble (ISCDG)*, Sept 2012, pp. 143–146.

[7] P. Lorenzi, R. Rao, and F. Irrera, "Forming kinetics in HfO_2-based RRAM cells," *IEEE Trans. on Electron Devices*, vol. 60, no. 1, pp. 438–443, 2013.

[8] A. Grossi, D. Walczyk, C. Zambelli, E. Miranda, P. Olivo, V. Stikanov, A. Feriani, J. Sune, G. Schoof, R. Kraemer, B. Tillack, A. Fox, T. Schroeder, C. Wenger, and C. Walczyk, "Impact of Intercell and Intracell Variability on Forming and Switching Parameters in RRAM Arrays," *IEEE Trans. on Electron Devices*, vol. 62, no. 8, pp. 2502–2509, Aug 2015.

[9] K. Morgan, R. Huang, S. Pearce, and C. de Groot, "The effect of atomic layer deposition temperature on switching properties of HfOx resistive RAM devices," in *IEEE Int. Symp. on Circuits and Systems (ISCAS)*, June 2014, pp. 432–435.

[10] H.-D. Kim, F. Crupi, M. Lukosius, A. Trusch, C. Walczyk, and C. Wenger, "Resistive switching characteristics of integrated polycrystalline hafnium oxide based one transistor and one resistor devices fabricated by atomic vapor deposition methods," *Journal of Vacuum Science and Technology B*, vol. 33, no. 5, pp. 052 204.1–052 204.5, 2015.

[11] A. Grossi, C. Zambelli, P. Olivo, E. Miranda, V. Stikanov, C. Walczyk, and C. Wenger, "Electrical characterization and modeling of pulse-based forming techniques in RRAM arrays," *Solid-State Electronics*, vol. 115, Part A, pp. 17 – 25, 2016. [Online]. Available: http://www.sciencedirect.com/science/article/pii/S0038110115002828

[12] A. Grossi, C. Zambelli, P. Olivo, E. Miranda, V. Stikanov, T. Schroeder, C. Walczyk, and C. Wenger, "Relationship among current fluctuations during forming, cell-to-cell variability and reliability in RRAM arrays," in *IEEE Int. Memory Workshop (IMW)*, May 2015, pp. 1–4.

[13] V. Iglesias, M. Porti, M. Nafra, X. Aymerich, P. Dudek, and G. Bersuker, "Dielectric breakdown in polycrystalline hafnium oxide gate dielectrics investigated by conductive atomic force microscopy," *Journal of Vacuum Science and Technology B*, vol. 29, no. 1, 2011.

[14] S. Balatti, S. Ambrogio, A. Cubeta, A. Calderoni, N. Ramaswamy, and D. Ielmini, "Voltage-dependent random telegraph noise (RTN) in HfOx resistive RAM," in *IEEE Int. Reliability Physics Symposium*, June 2014, pp. MY.4.1–MY.4.6.